Space weather and geomagnetic activity related to M6+ earthquakes recorded between 7 and 20 November 2017

Gabriele Cataldi[1], Daniele Cataldi[1-2], Valentino Straser[3]

(1) Radio Emissions Project (I). ltpaobserverproject@gmail.com
(2) Fondazione Permanente G. Giuliani - Onlus (I). daniele77c@hotmail.it
(3) Department of Science and Environment UPKL Brussel (B). valentino.straser@gmail.com

Abstract

Between 7 and 20 November 2017, ten high intensity seismic events (M6+) were recorded on our planet. The authors, analyzing the characteristics of solar ion flux and terrestrial geomagnetic activity, found that the ten potentially destructive seismic events were preceded by solar wind proton density increases and by increases in terrestrial geomagnetic activity.

Keywords: proton density increase, seismic precursors, solar activity, earthquake prevision, geomagnetic activity.

Introduction

The authors are engaged since 2012 in the monitoring of the solar ion flux density and the effects this has on the Earth's geomagnetic field as part of a research project (Radio Emissions Project) dedicated to monitoring and studying seismic precursors of electromagnetic type that it has set itself the goal of tracing a physical phenomenon of an electromagnetic nature that can be correlated with the M6+ global seismic activity [22]. Over the past nine years the authors have been able to identify a very reliable electromagnetic seismic precursor that always precedes potentially destructive seismic events: this seismic precursor is represented by a solar wind proton density increases, and has been defined by the authors as "Interplanetary Seismic Precursor" (ISP) as it is an electromagnetic physical phenomenon generated by the Sun that can be traced within the interplanetary space [3-16] [18-25]. In this study the authors will present the results obtained through the monitoring and analysis of the solar ion flux and the Earth's geomagnetic activity in the period from 5 and 20 November 2017: time interval in which 10 seismic events of strong intensity were recorded on a global scale (Fig. 1 and 2):

1. M6.5 Papua New Guinea earthquake, recorded on November 7, 2017 at 21:26:38 UTC (110,6km depth);
2. M6.0 Japan earthquake, recorded on November 9, 2017 at 07:42:11 UTC (12km depth);
3. M6.1 Ascension Island region earthquake, recorded on November 11, 2017 at 00:36:14 UTC (10km depth)
4. M7.3 Iraq earthquake, recorded on November 12, 2017 at 18:18:17 UTC (19km depth);
5. M6.5 Costa Rica earthquake, recorded on November 13, 2017 at 02:28:23 UTC (19,4km depth);
6. M6.4 China earthquake, recorded on November 17, 2021 at 22:34:19 UTC (8km depth);
7. M6.3 New Caledonia earthquake, recorded on November 19, 2017 at 09:25:48 UTC (14km depth);
8. M6.6 New Caledonia earthquake, recorded on November 19, 2017 at 15:09:02 UTC (13km depth);
9. M7.0 New Caledonia earthquake, recorded on November 19, 2017 at 22:43:29 UTC (10km depth);
10. M6.0 New Caledonia earthquake, recorded on November 20, 2017 at 00:09:23 UTC (10km depth);

All these seismic events occurred chronologically in two distinct time intervals: two seismic trains, each of which was preceded both by a solar wind proton density increase and by an increase in the Earth's geomagnetic activity. The increases in the Earth's geomagnetic field were correlated by the authors to the M6+ global seismic activity starting from 2010-2011 and have, for this reason, been defined as "Seismic Geomagnetic Precursors" (SGPs) [1-4] [9] [11-13] [15] [16] [18] [22-25]. The SGPs always follow the ISPs due to the coupling function between solar activity and the earth's magnetosphere.

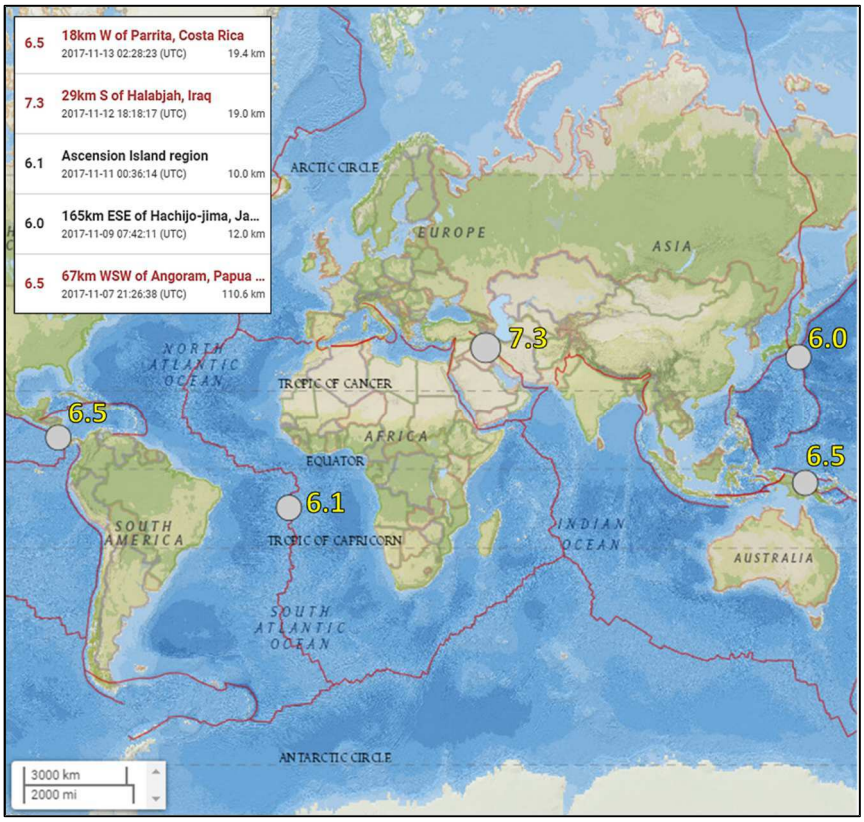

Fig. 1 – Seismic epicenter of M6+ earthquakes recorded between 7 and 13 November 2017 (first seismic train). The map above shows the seismic epicenter of five M6+ earthquakes recorded between 7 and 13 November 2017.
Credits: USGS, Radio Emissions Project.

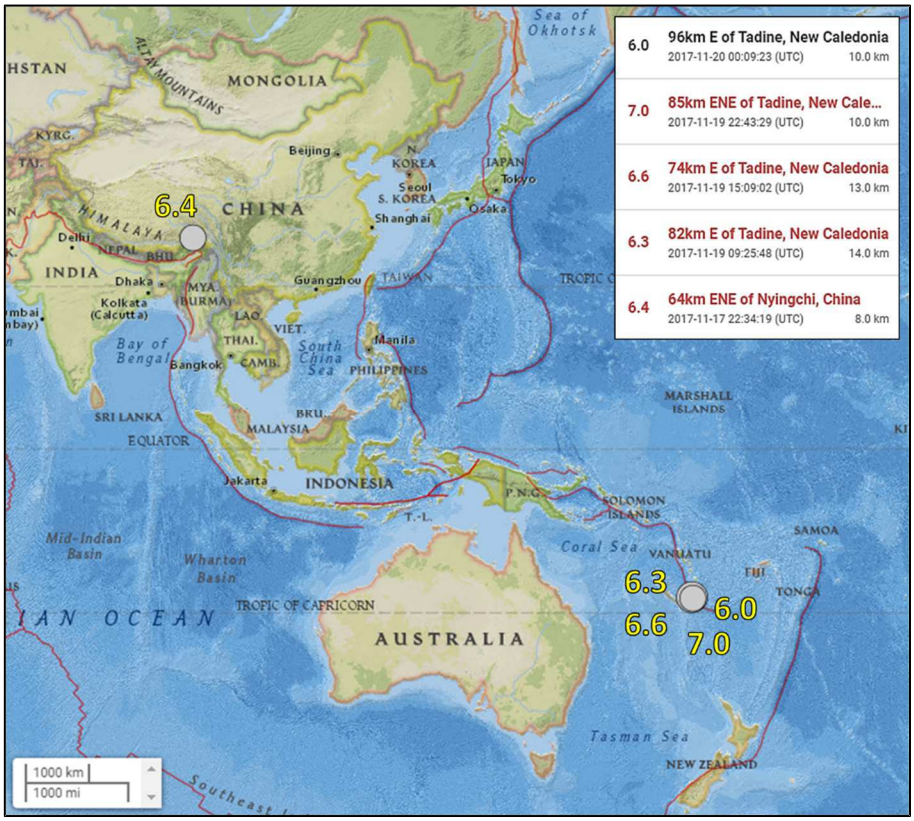

Fig. 2 – Seismic epicenter of M6+ earthquakes recorded between 17 and 20 November 2017 (second seismic train). The map above shows the seismic epicenter of five M6+ earthquakes recorded between 17 and 20 November 2017.
Credits: USGS, Radio Emissions Project.

Data analysis

To understand if the two M6+ seismic trains were preceded by a solar wind proton density increase, the authors analyzed the modulation of the solar ion flux between 5 and 20 November 2017; and in particular the proton energy fractions: 761-1220 KeV; 1060-1900 KeV and 310-580 KeV (Fig. 3 and 4). To this was added the monitoring of the Earth's geomagnetic activity as it is susceptible to variations in the solar ion flux.

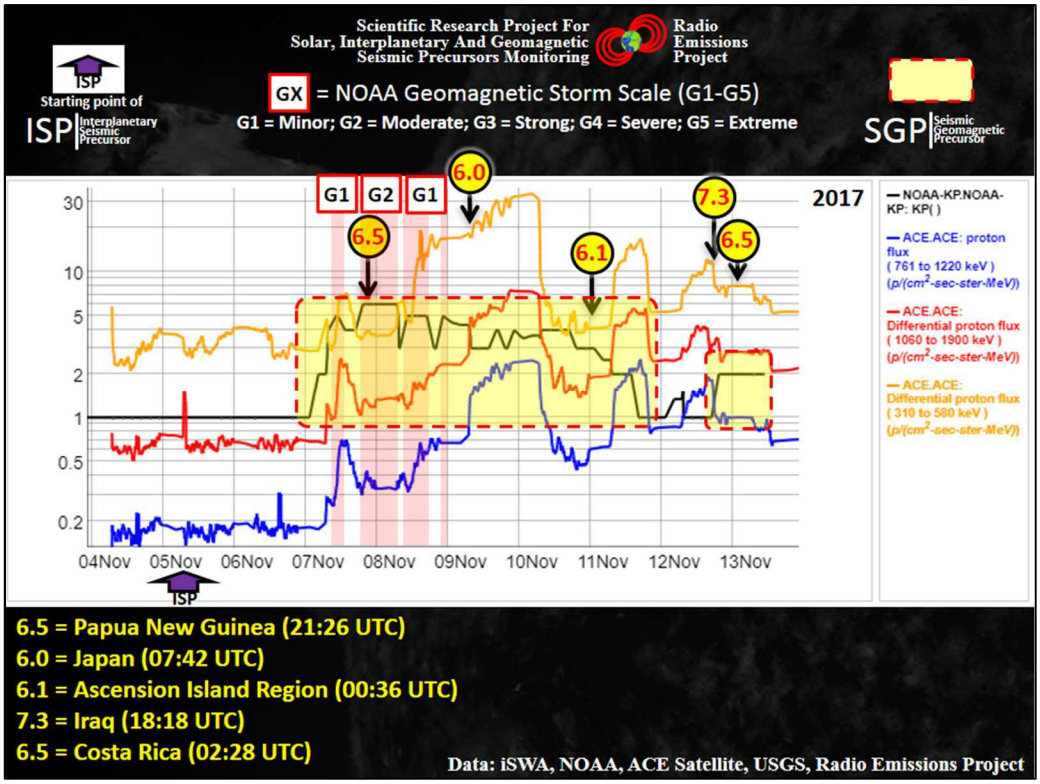

Fig. 3 – Variation in solar ion flux and Earth's geomagnetic activity related to the M6+ global seismic activity recorded between 7 and 13 November 2017 (first seismic train). Graph contains the data on the variation of solar wind proton density (blu, red and yellow lines) recorded between 4 and 13 November 2017 recorded at the L1 Lagrange point by Advanced Composition Explorer (ACE) satellite; the variation of Kp Index and the temporal markers (black vertical arrows) of M6+ earthquakes recorded in the same period. The vertical purple arrow represents the beginning of the "gradual" proton density increase (beginning of Interplanetary Seismic Precursor). The yellow areas surrounded by the red dashed line indicates increases of Kp Index (black line) that preceded the M6+ earthquakes (Geomagnetic Seismic Precursor). The data on the proton density variation and the Kp Index were provided by iSWA. iSWA is a flexible, turn-key, Web-based dissemination system for NASA-relevant space weather information that combines forecasts based on the most advanced space weather models with concurrent space environment information. The data on seismic activity were provided by United States Geological Survey (USGS).
Credits: iSWA, USGS, Radio Emissions Project.

The analysis of the solar ion flux showed that a solar wind proton density increase (Interplanetary Seismic Precursor or ISP) preceded the first M6+ seismic train consisting of the following earthquakes:

1. M6.5 Papua New Guinea earthquake, recorded on November 7, 2017 at 21:26:38 UTC (110,6km depth);
2. M6.0 Japan earthquake, recorded on November 9, 2017 at 07:42:11 UTC (12km depth);
3. M6.1 Ascension Island region earthquake, recorded on November 11, 2017 at 00:36:14 UTC (10km depth)
4. M7.3 Iraq earthquake, recorded on November 12, 2017 at 18:18:17 UTC (19km depth);
5. M6.5 Costa Rica earthquake, recorded on November 13, 2017 at 02:28:23 UTC (19,4km depth);

and generated an intense geomagnetic perturbation which began on November 7, 2017 and ended on November 11, 2017 (Seismic Geomagnetic Precursor or SGP): within this time interval, 4 geomagnetic storms were recorded with a grade (NOAA G Scale, Fig. 3) of:

1) G1 – recorded on November 7, 2017;

2) G2 – recorded between 7 and 8 November 2017;
3) G1 – recorded during the first part of November 8, 2017;
4) G1 – recorded during the second part of November 8, 2017.

The first seismic event (M6.5 Papa New Guinea earthquake) was recorded during the G1 grade geomagnetic storm recorded on November 7, 2017; the second seismic event (M6.0 Japan earthquake) was recorded 7 hours after the end of the third geomagnetic storm, while the remaining M6+ seismic events were recorded between 11 and 13 November 2017.

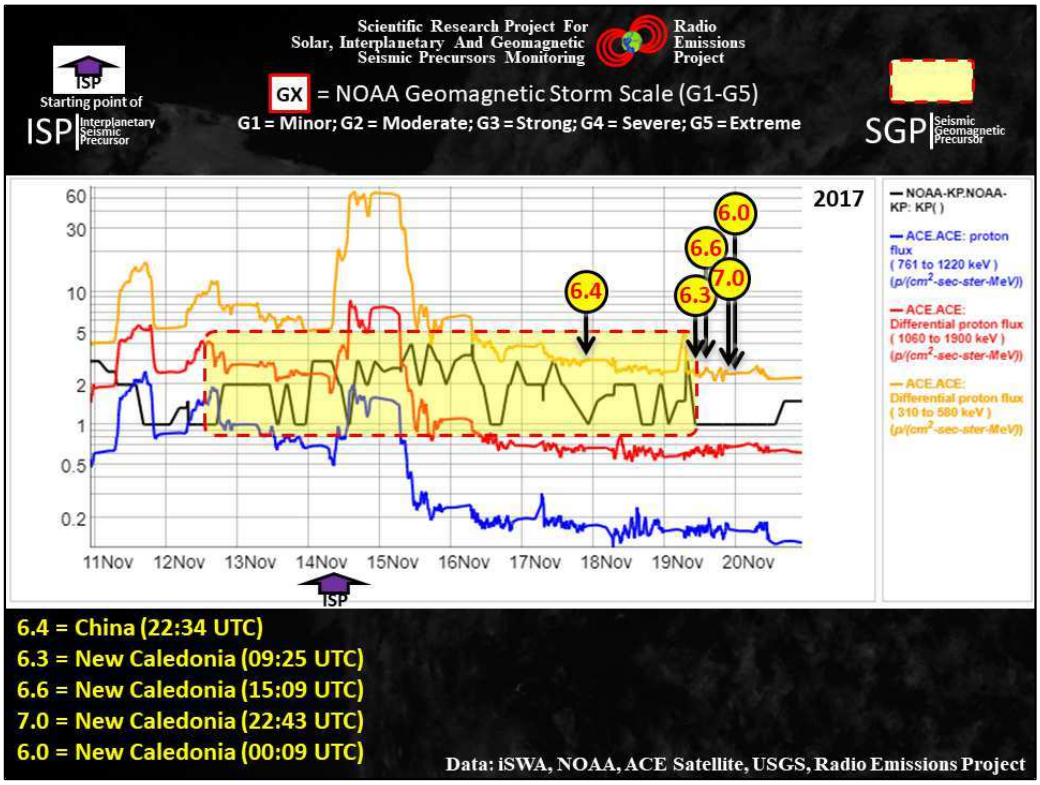

Fig. 4 – Variation in solar ion flux and Earth's geomagnetic activity related to the M6+ global seismic activity recorded between 17 and 20 November 2017 (second seismic train). Graph contains the data on the variation of solar wind proton density (blu, red and yellow lines) recorded between 11 and 20 November 2017 recorded at the L1 Lagrange point by Advanced Composition Explorer (ACE) satellite; the variation of Kp Index and the temporal markers (black vertical arrows) of M6+ earthquakes recorded in the same period. The vertical purple arrow represents the beginning of the "gradual" proton density increase (beginning of Interplanetary Seismic Precursor). The yellow areas surrounded by the red dashed line indicates increases of Kp Index (black line) that preceded the M6+ earthquakes (Geomagnetic Seismic Precursor). The data on the proton density variation and the Kp Index were provided by iSWA. iSWA is a flexible, turn-key, Web-based dissemination system for NASA-relevant space weather information that combines forecasts based on the most advanced space weather models with concurrent space environment information. The data on seismic activity were provided by United States Geological Survey (USGS).
Credits: iSWA, USGS, Radio Emissions Project.

The analysis of the solar ion flux showed that a solar wind proton density increase (Interplanetary Seismic Precursor or ISP) preceded the second M6+ seismic train consisting of the following earthquakes:

1. M6.4 China earthquake, recorded on November 17, 2021 at 22:34:19 UTC (8km depth);
2. M6.3 New Caledonia earthquake, recorded on November 19, 2017 at 09:25:48 UTC (14km depth);
3. M6.6 New Caledonia earthquake, recorded on November 19, 2017 at 15:09:02 UTC (13km depth);
4. M7.0 New Caledonia earthquake, recorded on November 19, 2017 at 22:43:29 UTC (10km depth);
5. M6.0 New Caledonia earthquake, recorded on November 20, 2017 at 00:09:23 UTC (10km depth);

generating a geomagnetic perturbation (started in the second half of November 12, 2017; Seismic Geomagnetic Precursor or SGP; Fig. 4) that preceded all earthquakes.

All ten seismic events analyzed in this study were preceded by a solar wind proton density increase and, in this specific case, by two increases that partially overlapped (Fig. 3 and 4). This detail can also be understood by analyzing the variation curve of the solar wind speed (Fig. 5).

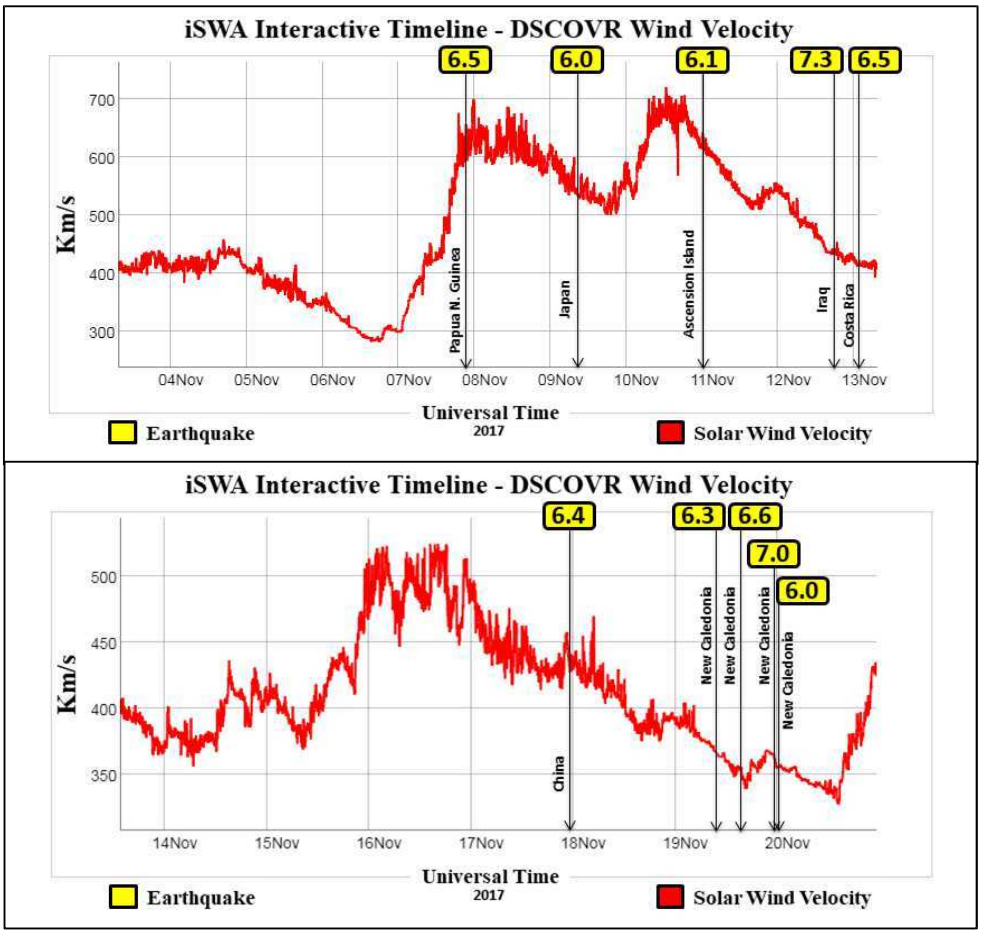

Fig. 5 – Solar wind velocity correlated to M6+ earthquakes recorded between 7 and 20 November 2017. The graph shows the variation of solar wind velocity recorded between 3 and 20 November 2017 by Deep Space Climate Observatory (DSCOVR) Satellite, in orbit at L1 Lagrange point. Analyzing the variation curve, it is possible to understand that the ten M6+ earthquakes was preceded by an increase of the solar wind speed. In the top portion of the graph is visible the trend of the solar wind speed correlated to the first seismic train; in the lower portion of the graph is visible the trend of the solar wind speed correlated to the second seismic train. The black vertical arrow shows the temporal marker of the M6+ earthquakes.
Credits: iSWA, Radio Emissions Project.

According to the data visible in Fig. 5 it is evident that the first seismic train was preceded by an increase in the solar wind speed which started on November 6, 2017; while the second seismic train was preceded by an increase in the solar wind speed which started on November 14, 2017.

Conclusions

Also in this case we are faced with a series of scientific evidence that it is impossible not to consider clear and genuine. Over the past ten years, the authors have collected a considerable amount of data to support the link that exists between solar activity and M6+ global seismic activity [1-25]. In the coming months and in the years to come, the amount of data supporting this connection will be ever greater and it is evident that today there is a need for an important step change in research focused on the development of new models capable of predicting early when a potentially destructive earthquake will strike. The authors were able to develop a method capable of establishing when, on a global scale, a resumption of M6+ seismic activity is expected by identifying an electromagnetic seismic precursor that can be monitored through the use of artificial satellites. The hope of the authors is that very soon this method will be seriously considered by the international scientific community.

Credits

[1] G. Cataldi, D. Cataldi, V. Straser. (2013). Variations Of Terrestrial Geomagnetic Activity Correlated To M6+ Global Seismic Activity. EGU (European Geosciences Union) 2013, General Assembly, Seismology Section (SM3.1), Earthquake precursors, bio-anomalies prior to earthquakes and prediction, Geophysical Research Abstracts, Vol. 15. EGU2013-2617, Vienna, Austria. Harvard-Smithsonian Center for Astrophysics, High Energy Astrophysics Division, SAO/NASA Astrophysics Data System.

[2] G. Cataldi, D. Cataldi and V. Straser. (2014). Earth's magnetic field anomalies that precede the M6+ global seismic activity. European Geosciences Union (EGU) General Assembly 2014, Geophysical Research Abstract, Vol. 16, EGU2014-1068, Vienna, Austria. Natural Hazard Section (NH4.3), Electro-magnetic phenomena and connections with seismo-tectonic activity, Harvard-Smithsonian Center for Astrophysics, High Energy Astrophysics Division, SAO/NASA Astrophysics Data System.

[3] T. Rabeh, G. Cataldi, V. Straser. (2014). Possibility of coupling the magnetosphere–ionosphere during the time of earthquakes. European Geosciences Union (EGU) General Assembly 2014, Geophysical Research Abstract, Vol. 16, EGU2014-1067, Vienna, Austria. Natural Hazard Section (NH4.3), Electro-magnetic phenomena and connections with seismo-tectonic activity. Harvard-Smithsonian Center for Astrophysics, High Energy Astrophysics Division, SAO/NASA Astrophysics Data System.

[4] V. Straser, G. Cataldi. (2014). Solar wind proton density increase and geomagnetic background anomalies before strong M6+ earthquakes. Space Research Institute of Moscow, Russian Academy of Sciences, MSS-14. 2014. Moscow, Russia. pp280-286.

[5] V. Straser, G. Cataldi. (2015). Solar wind ionic variation associated with earthquakes greater than magnitude M6.0. New Concepts in Global Tectonics Journal, V. 3, No. 2, June 2015, Australia. P.140-154.

[6] G. Cataldi, D. Cataldi, V. Straser. (2015). Solar wind proton density variations that preceded the M6+ earthquakes occurring on a global scale between 17 and 20 April 2014. European Geosciences Union (EGU) General Assembly 2015, Vienna, Austria. Natural Hazard Section (NH5.1), Sea & Ocean Hazard - Tsunami, Geophysical Research Abstract, Vol. 17, EGU2015-4157-2, Harvard-Smithsonian Center for Astrophysics, High Energy Astrophysics Division, SAO/NASA Astrophysics Data System.

[7] G. Cataldi, D. Cataldi, V. Straser. (2015). Solar wind ion density variations that preceded the M6+ earthquakes occurring on a global scale between 3 and 15 September 2013. European Geosciences Union (EGU) General Assembly 2015, Geophysical Research Abstract, Vol. 17, EGU2015-4581, Vienna, Austria. Natural Hazard Section (NH5.1), Sea & Ocean Hazard - Tsunami, Harvard-Smithsonian Center for Astrophysics, High Energy Astrophysics Division, SAO/NASA Astrophysics Data System.

[8] G. Cataldi, D. Cataldi, V. Straser. (2015). Solar wind proton density variations that preceded the M6,1 earthquake occurred in New Caledonia on November 10, 2014. European Geosciences Union (EGU) General Assembly 2015, Geophysical Research Abstract, Vol. 17, EGU2015-4167, Vienna, Austria. Natural Hazard Section (NH5.1), Sea & Ocean Hazard - Tsunami, Harvard-Smithsonian Center for Astrophysics, High Energy Astrophysics Division, SAO/NASA Astrophysics Data System.

[9] V. Straser, G. Cataldi, D. Cataldi. (2015). Solar wind ionic and geomagnetic variations preceding the Md8.3 Chile Earthquake. New Concepts in Global Tectonics Journal, V. 3, No. 3, September 2015, Australia. P.394-399.

[10] G. Cataldi, D. Cataldi, V. Straser. (2016). Solar activity correlated to the M7.0 Japan earthquake occurred on April 15, 2016. New Concepts in Global Tectonics Journal, V. 4, No. 2, pp202-208, June 2016.

[11] G. Cataldi, D. Cataldi, V. Straser. (2016). Tsunami related to solar and geomagnetic activity. European Geosciences Union (EGU) General Assembly 2016, Natural Hazard Section (NH5.6), Complex modeling of earthquake, landslide, and volcano tsunami sources. Geophysical Research Abstract, Vol. 18,

EGU2016-9626, Vienna, Austria. Harvard-Smithsonian Center for Astrophysics, High Energy Astrophysics Division, SAO/NASA Astrophysics Data System.

[12] G. Cataldi, D. Cataldi, V. Straser. (2017). SELF-VLF electromagnetic signals and solar wind proton density variations that preceded the M6.2 Central Italy earthquake on August 24, 2016. International Journal of Modern Research in Electrical and Electronic Engineering, Vol. 1, No. 1, 1-15. DOI: 10.20448/journal.526/2017.1.1/526.1.1.15.Harvard-Smithsonian Center for Astrophysics, High Energy Astrophysics Division, SAO/NASA Astrophysics Data System.

[13] G. Cataldi, D. Cataldi, V. Straser. (2017). Solar and Geomagnetic Activity Variations Correlated to Italian M6+ Earthquakes Occurred in 2016. European Geosciences Union (EGU), General Assembly 2017. Geophysical Research Abstracts Vol. 19, EGU2017-3681, 2017. Seismology (SM1.2)/Natural Hazards (NH4.7)/Tectonics & Structural Geology (TS5.5) The 2016 Central Italy Seismic sequence: overview of data analyses and source models.Harvard-Smithsonian Center for Astrophysics, High Energy Astrophysics Division, SAO/NASA Astrophysics Data System.

[14] G. Cataldi, D. Cataldi, V. Straser. (2017). Solar wind proton density increase that preceded Central Italy earthquakes occurred between 26 and 30 October 2016. European Geosciences Union (EGU), General Assembly 2017. Geophysical Research Abstracts Vol. 19, EGU2017-3774, 2017. Seismology (SM1.2)/Natural Hazards (NH4.7)/Tectonics & Structural Geology (TS5.5) The 2016 Central Italy Seismic sequence: overview of data analyses and source models. Harvard-Smithsonian Center for Astrophysics, High Energy Astrophysics Division, SAO/NASA Astrophysics Data System.

[15] V. Straser, G. Cataldi, D. Cataldi. (2017). Solar and electromagnetic signal before Mexican Earthquake M8.1, September 2017. New Concepts in Global Tectonics Journal, V. 5, No. 4, December 2017. pp600-609.

[16] G. Cataldi, D. Cataldi, V. Straser. (2017). Solar and Geomagnetic Activity Variations Correlated to Italian M6+Earthquakes Occurred in 2016. EGU General Assembly 2017. EGU2017-3681, Vol. 19.

[17] G. Cataldi, D. Cataldi, V. Straser. (2019). Solar wind ionic density variations related to M6+ global seismic activity between 2012 and 2018. European Geosciences Union (EGU) General Assembly 2019, Short-term Earthquake Forecast (StEF) and multy-parametric time-Dependent Assessment of Seismic Hazard (t-DASH) (NH4.3/AS4.62/EMRP2.40/ESSI1.7/Gi2.13/SM3.9), General Contribution on Earthquakes, Earth Structure, Seismology (SM1.1), Geophysical Research Abstract, Vol. 21, EGU2019-3067, 2019, Vienna, Austria. Harvard-Smithsonian Center for Astrophysics, High Energy Astrophysics Division, SAO/NASA Astrophysics Data System.

[18] G. Cataldi. (2020). Precursori Sismici – Monitoraggio Elettromagnetico. Kindle-Amazon, ISNB: 9798664537970. ASIN Code: B08CPDBGX9.

[19] G. Cataldi, D. Cataldi, V. Straser. (2019). Wolf Number Related To M6+ Global Seismic Activity. New Concepts in Global Tectonics Journal, Volume 7, Number 3, December 2019, pp. 178-186.

[20] V. Straser, G. Cataldi, D. Cataldi. (2020). The Space Weather Related to the M7+ Seismic Activity Recorded on a Global Scale between 28 January and 25 March 2020. Acta Scientific Agriculture 4.12 (2020): 55-62.

[21] G. Cataldi, V. Straser, D. Cataldi. (2020). Space Weather related to potentially destructive seismic activity recorded on a global scale. New Concepts in Global Tectonics Journal. Vol.8, No.3, pp.233-253, December 2020. ISSN 2202-0039.

[22] G. Cataldi. (2021). Radio Emissions Project – A new approach to seismic prediction. Kindle-Amazon, ISNB: 9798709593411.

[23] G. Cataldi, D. Cataldi, V. Straser. (2021). Space weather and geomagnetic activity related to the Japan M7.1 earthquake recorded on February 13, 2021. New Concepts in Global Tectonics Journal, Vol. 9, No. 1, pp.16-23. March 2021.

[24] G. Cataldi, D. Cataldi, V. Straser. (2021). Space weather and geomagnetic activity related to the Chilean M6.7 earthquake recorded on February 3, 2021. New Concepts in Global Tectonics Journal, Vol. 9, No. 1, pp.3-9. March 2021.

[25] G. Cataldi, D. Cataldi, V. Straser. (2021). Space weather and geomagnetic activity related to M6+ global seismic activity recorded on February 7, 2021. New Concepts in Global Tectonics Journal, Vol. 9, No. 1, pp.24-30. March 2021.